

# Regional Heterogeneity of Length–Tension Relationships in Rat Lymph Vessels

Anatoliy A. Gashev, M.D., Ph.D., D.Med.Sci.,<sup>1</sup> Rong-Zhen Zhang, M.D.,<sup>2</sup>  
Mariappan Muthuchamy, Ph.D.,<sup>1</sup> David C. Zawieja, Ph.D.,<sup>1</sup> and Michael J. Davis, Ph.D.<sup>3</sup>

## Abstract

**Background:** Heterogeneity of the length–tension relationships in lymph vessels has never been evaluated systematically.

**Methods and Results:** In this study we measured the length–tension relationships in lymph vessels from three different regions of the rat: thoracic duct, cervical, and femoral lymph vessels, and compared the results to our previous measurements of rat mesenteric lymph vessels. We performed isometric force measurements on activated and passive lymph vessel segments using a small-vessel wire myograph. We found that all groups of vessels had relatively broad plateaus in their active tension versus length relationships, suggesting that they are adapted to generate near-maximal tensions over a relatively wide range of preloads (at least 0.85–1.05  $L_0$ ). Thoracic duct exhibited the flattest active tension curve, particularly for peak active tension, in which there was less than a 5% change in peak active tension from 0.75 to 1.30 of optimal length. Femoral lymph vessels were able to withstand the highest estimated pressures, followed by mesenteric and cervical vessels and then thoracic duct.

**Conclusions:** We conclude that lymph vessels effectively adapt their contractile force to the particular hydrodynamic conditions (transmural pressures and intraluminal flows) that exist in different regions of the lymphatic system.

## Introduction

THE LYMPHATIC SYSTEM is critical to fluid homeostasis. The lymphatic capillary network serves as a compartment to absorb tissue fluid through primary lymphatic valves created by the overlap of endothelial cells in the walls of initial lymphatics.<sup>1,2</sup> Lymph accumulates in the initial lymphatics, but the resulting hydrostatic pressure is insufficiently strong to maintain effective lymph transport through the collecting lymphatics and lymph nodes to the thoracic duct and great veins (for review see, Ref. 3). Effective lymph transport from peripheral to central vessels requires the contractions of one or more layers of lymphatic muscle cells in the walls of the collecting lymph vessels. The presence of secondary luminal valves,<sup>2</sup> which divide those vessels into chambers—lymphangions,<sup>4</sup> serve to minimize the back-flow of lymph.<sup>3,5–7</sup> Therefore, the contractile force of the muscular lymph vessels,

which serve as the transporting lymphatic compartment, is critical for fluid homeostasis in the majority of mammals, including humans.

In lymphatic muscle, as in all muscle, active force development depends on the initial muscle cell length (preload) as well as the load against which the muscle must work after it is activated (afterload). For lymph vessels, preload is determined by end-diastolic wall stretch due to the diastolic filling of the lymphangion;<sup>8–11</sup> afterload is determined by the moment-to-moment pressure fluctuations in the downstream lymphangion and, in a dependent extremity, by the prevailing gravitational hydrostatic load. Lymphangions can be described as self-regulating pumps, which are constantly adjusting their force generation to account for variable combinations of different preloads and afterloads.<sup>3</sup>

In the majority of local lymphatic networks, the existing net pressure gradient opposes lymph flow most of the time so that

<sup>1</sup>Department of Systems Biology and Translational Medicine, College of Medicine, Texas A&M Health Science Center, Temple/College Station, Texas.

<sup>2</sup>Department of Pathology, University of Texas Health Sciences Center, Houston, Texas.

<sup>3</sup>Department of Medical Pharmacology and Physiology, University of Missouri, Columbia, Missouri.

This work was supported in part by the National Institutes of Health Grants (NIH RO1 HL-075199, HL-070308, HL-089784, AG-030578, and HL-094269).

lymphangions must support effective lymph flow by active phasic pumping.<sup>3</sup> In contrast, lymph vessels located above the level of the chest (particularly in bipedal humans) are exposed to the opposite situation where gravitational forces support net lymph flow.<sup>12</sup> We demonstrated previously that such variability in local hydrodynamic conditions leads to regional variability in both pressure- and flow-dependent reactions of lymphatic vessels.<sup>13</sup>

Based on our previous work, we proposed that regional heterogeneity in the sensitivity of lymph vessels to changes in transmural pressure/stretch reflects differences in the force-generating ability of the lymphatic muscle cells. To test this idea, it is important to measure the basic length-tension (L-T) relationships of lymph vessels from different regions of the body<sup>13</sup> to compare these relationships among the different vessel types and to analyze them in the context of the pressure-induced contractile responses of similar vessels obtained under isobaric conditions. To accomplish this goal, we used a small vessel wire myograph to measure the L-T relationships of the thoracic duct and collecting lymphatic vessels from cervical and femoral regions of the rat under isometric conditions and compared them to the L-T relationship previously determined for rat mesenteric vessels.

## Materials and Methods

### *Isolated vessel preparation*

Male Sprague-Dawley rats (200–300 g) were used for all experiments. All animal protocols conformed to institutional and federal guidelines.

To isolate segments of the thoracic duct, rats were euthanized with pentobarbital sodium (120 mg/kg body weight IP). The animal was positioned on its back, the ventral chest wall was opened by lateral incision, and the sternum and approximately half of the ribs were excised. The inferior vena cava was ligated and cut close to the diaphragm. The lungs and heart were pulled to the left side of the animal to expose the thoracic duct between the aorta and vertebral column. The thoracic duct was then carefully cleared of all surrounding tissue under a dissecting microscope. Extreme caution was used at all times to prevent direct contact with the thoracic duct, thereby reducing the likelihood of damage. The segment of interest was kept moist for the period of dissection using physiological saline solution (PSS) containing the following (in mM): 145.0 NaCl, 4.7 KCl, 2.0 CaCl<sub>2</sub>, 1.17 MgSO<sub>4</sub>, 1.2 NaH<sub>2</sub>PO<sub>4</sub>, 0.02 EDTA, 5.0 glucose, 2.0 sodium pyruvate, 3.0 3-(*N*-morpholino) propanesulfonic acid, and 1 g/100 ml purified bovine serum albumin. Sections of thoracic duct ~1 cm long were used for experiments.

To isolate segments of cervical lymph vessels, rats were anesthetized with pentobarbital (60 mg/kg body weight IP). The skin was removed from the entire ventral surface of the neck. Underlying fascia and superficial muscles were dissected in the area near the confluence of the external and internal jugular veins. Cervical lymph vessels were identified as comparatively large lymphatic trunks between the internal and external jugular veins located on the cephalic side of their confluence, deeper than the level of veins. These lymph vessels formed a sharp angle with the external jugular vein and were sometimes found under the external jugular vein. Sections of cervical lymph vessels ~1 cm in length were dissected and used for experiments. After isolation of

the vessels, the rat was euthanized with pentobarbital (120 mg/kg body weight IP.)

For isolation of segments of femoral lymph vessels, anesthesia and euthanasia procedures were the same as those used to obtain the cervical lymph vessels. The skin was removed from the internal surface of the thigh. Superficial fascia and muscle layers were quickly removed to provide access to the area of connections between the femoral artery, the internal iliac artery, and the artery of the deferent duct. Suitable lymph vessels were found between these arteries. After careful cleaning in situ, sections of the femoral lymph vessels ~1 cm long were dissected and used for experiments.

After dissection, the lymph vessel of interest was cut into 2-mm long segments and transferred to a wire myograph chamber.

### *Mounting lymphatic segments*

Isometric experiments were performed using a single-channel wire myograph (Danish Myo, model 310A; J.P. Trading, Aarhus, Denmark). In PSS at room temperature, the vessel segment was threaded onto a suitable length of stainless steel wire (diameter = 40  $\mu$ m for thoracic duct; 25  $\mu$ m for other lymph vessels) and the wire was secured to one jaw of the myograph. The second wire was passed gently through the vessel lumen and then anchored to the other jaw of the myograph. An adjustable micrometer was used to separate the jaws and stretch the vessel between the two parallel wires. A calibrated force transducer (Danish Myo, J.P. Trading) measured forces between 0 and 40 mN. The force output was digitized with a PCI-6030e A-D card and interface (National Instruments, Austin, TX) and displayed using a Pentium 4 computer running a custom program written in LabVIEW (National Instruments). Data were typically collected at 10 Hz. After each segment was mounted in the myograph, the bath temperature was raised to  $37 \pm 0.1^\circ\text{C}$ .

### *Microscope system*

The mounted segment was transferred to the stage of an inverted microscope (Olympus model CK40-F1000) coupled to a CCD camera (Hitachi Denshi, model PK-M2U). A video micrometer (Microcirculation Research Institute, Texas A&M University, TX) was used to measure inner and outer diameters, and the video was recorded using a digital VCR (Panasonic, model DMR-E85H). The thickness of the wall was measured at several sites along the vessel at each level of preload for later determination of wall stress.

### *Experimental protocols*

Each vessel was equilibrated for ~1 h in PSS, with the solution being changed once during the equilibration period. Starting from a completely unloaded state, the circumferential length was slowly increased in a stepwise manner by manual adjustment of the distance between the jaws. After a stable level of force was achieved for ~2 min, the vessel was maximally activated with  $1 \cdot 10^{-6}$  M Substance P in K•PSS where equimolar KCl was substituted for NaCl in PSS (K•PSS). The time course of active force development was then recorded for 5–10 min. After washing in PSS twice, the vessels were returned to a completely unloaded state, and the force transducer was re-zeroed. After ~5 min, the passive length was

increased and the activation protocol repeated. This procedure was repeated until no further increase in active force ( $F_{max}$ ) was recorded. The passive and total length-force relations were then determined.

Statistical differences were determined by two-way ANOVA or paired Student's *t*-test and considered significant at  $p \leq 0.05$ .

## Results

Table 1 summarizes the passive and active mechanical properties of the three lymph vessel types; 12 vessels were studied from each region.

Figure 1 summarizes the length-tension (L-T) relationships for lymph vessels from the three different regions. To facilitate comparisons with our previously published data on the L-T relationship for rat mesenteric lymph vessels using the same method, we have re-plotted the mean data from the mesenteric vessels in panels G and H (from Ref. 11). The diameter of mesenteric lymph vessels at optimal preload was  $149.1 \pm 4.1 \mu\text{m}$ .<sup>11</sup> Panels A, C, E, and G show tension as a function of initial length for the peak of force development after the vessel was activated with SP in K•PSS; force typically peaked about

15–30 sec after addition of activating solution. Panels B, D, F, and H show tension as a function of initial length for the plateau phase of force development after the vessel was activated; these measurements were typically made 90–120 sec after activation. In each panel, the curve represented by open squares describes the relationship between passive wall tension and length, in which tension = force / (2 • segment length). The internal circumference of the vessel ( $L$ ) was calculated as the wire circumference plus 2 times the wire diameter plus 2 times the distance between the inner edges of the wire.<sup>11,14</sup>  $L$  was normalized to the optimal internal circumference ( $L_0$ ) at which vessels generated maximal active force ( $F_{max}$ ). The curve represented by filled squares describes the total length-tension relationship. The difference between the two curves (dashed lines) represents the active tension developed at each preload.

A few interesting differences between the vessels were notable. Peak active tension was comparable between cervical, femoral, and mesenteric lymph vessels; however, peak active tension for thoracic duct was ~55% greater than for the other vessels. The plateau active tensions were comparable between cervical and femoral lymph vessels, plateau active tension in thoracic duct was ~50% higher, and plateau active tension in mesenteric lymph vessels was intermediate between thoracic duct and the other vessels. All vessels had relatively broad plateaus in their active tension versus length relationships, suggesting that they could generate near-maximal tensions over a wide range of preloads ( $0.85$ – $1.05 L_0$ ). Thoracic duct exhibited the flattest active tension curve, particularly for peak active tension (<5% change in peak active tension from  $0.75$  to  $1.30 L_0$ ), whereas the corresponding curve was steepest for mesenteric lymph vessels.

The length-tension relationships of the passive and activated vessels were used to calculate the pressures at which each vessel would produce maximal active tension. Circular geometry was assumed, which is probably a valid assumption at normalized lengths  $> 0.6$  given the calculated pressure ranges associated with active force development. Figure 2 summarizes the calculated distending pressures for the three vessel types as a function of normalized diameter ( $D/D_0$ ), where  $D$  and  $D_0$  were calculated from  $L$  and  $L_0$ . Here, pressure is the equivalent intraluminal pressure required to sustain an isometric contraction in a cannulated, pressurized vessel of the same normalized diameter.<sup>14</sup> The equivalent pressure under isometric conditions was calculated using the Laplace equation: pressure = tension / (internal circumference /  $2\pi$ ). Maximal active pressure was calculated by subtracting the passive curve (open squares) from the total curve (filled squares). This represents an estimate of the pressure required to maintain a pressurized vessel isometric during maximal activation with  $1 \cdot 10^{-6}$  M SP in K•PSS. The active pressure-diameter relationships of all three types of vessels were non-linear and convex to the diameter axis. Femoral lymph vessels were able to withstand the highest pressures, followed by mesenteric and cervical vessels, and then thoracic duct.

Figure 3 compares wall stress as a function of initial length for the four lymph vessels. Again, previously published mean data from mesenteric lymph vessels<sup>11</sup> are shown in panels G and H for comparison. To compare the mechanical properties of vessels with remarkably different sizes (see Table 1), the contractile force was normalized to the smooth muscle mass, as reflected by the medial wall thickness.<sup>15,16</sup> Wall thickness data were obtained from direct dimensional measurements during

TABLE 1. MECHANICAL CHARACTERISTICS OF RAT LYMPH VESSELS

	<i>Thoracic Duct</i>	<i>Cervical</i>	<i>Femoral</i>
Diameter, $D_0$ ( $\mu\text{m}$ )	$404.5 \pm 10.1$	$236.1 \pm 9.5$	$203.0 \pm 10.7$
Number	12	12	12
Thickness of the wall of vessels ( $\mu\text{m}$ )	$10.8 \pm 0.9$	$8.1 \pm 0.6$	$7.8 \pm 0.5$
Volume of the wall of vessels ( $\mu\text{m}^2$ )	13,383	9,859	8,235
Passive tension at $L_0$ (mN/mm)	$0.13 \pm 0.01$	$0.13 \pm 0.01$	$0.15 \pm 0.01$
Maximal peak active tension (mN/mm)	$0.59 \pm 0.03$	$0.37 \pm 0.03$	$0.39 \pm 0.03$
Maximal plateau active tension (mN/mm)	$0.36 \pm 0.03$	$0.15 \pm 0.03$	$0.51 \pm 0.01$
Passive pressure at $R_0$ (cm H <sub>2</sub> O)	$6.4 \pm 0.2$	$11.1 \pm 0.2$	$15.6 \pm 0.9$
Maximal peak active pressure (cm H <sub>2</sub> O)	$36.3 \pm 2.9$	$35.4 \pm 1.9$	$39.4 \pm 2.4$
Maximal plateau active pressure (cm H <sub>2</sub> O)	$17.1 \pm 1.3$	$12.9 \pm 1.7$	$14.8 \pm 1.1$
Passive stress at $R_0$ ( $10^5$ N/m <sup>2</sup> )	$0.11 \pm 0.01$	$0.07 \pm 0.01$	$0.20 \pm 0.01$
Maximal peak active stress ( $10^5$ N/m <sup>2</sup> )	$0.63 \pm 0.07$	$0.50 \pm 0.07$	$0.51 \pm 0.05$
Maximal plateau active stress ( $10^5$ N/m <sup>2</sup> )	$0.38 \pm 0.05$	$0.21 \pm 0.05$	$0.20 \pm 0.02$

Values are means  $\pm$  SEM. Values of tension, pressure, and stress were calculated from the basal force reading on the myograph. The optimal internal circumference ( $L_0$ ) at which vessels generated maximal active force ( $F_{max}$ ) was calculated from the distance between the wires plus wire diameter, with the assumption of elliptical geometry.  $D_0$  and  $R_0$  corresponding to the optimal diameter and radius were respectively measured at  $L_0$ .

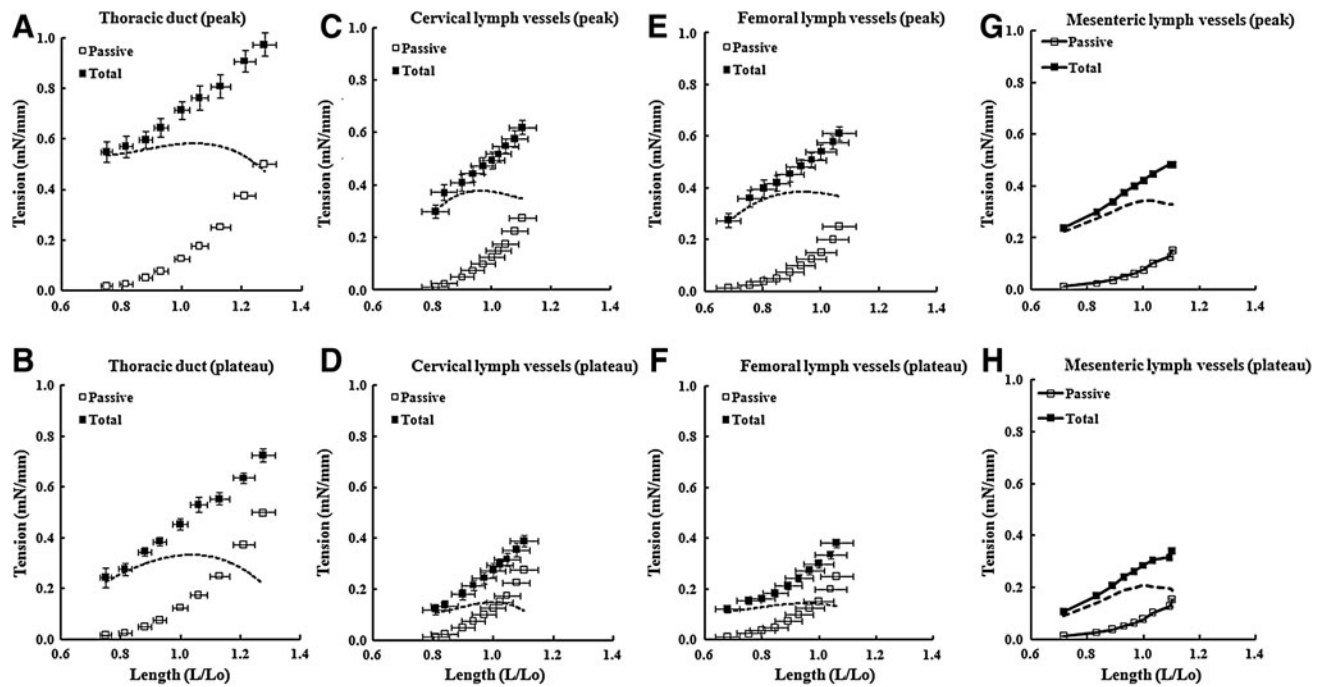


FIG. 1. Length-tension relationships for lymph vessels from four different regions.  $\square$ , Tension in passive vessels;  $\blacksquare$ , tension in activated vessels (total tension). The active tension (*dashed line*) was obtained by subtracting the passive curve from the total tension curve.  $L/L_0$ , length normalized to optimal internal circumference. Error bars,  $\pm$ SEM. Data from mesenteric lymph vessels is re-plotted from Ref. 11 for comparison.

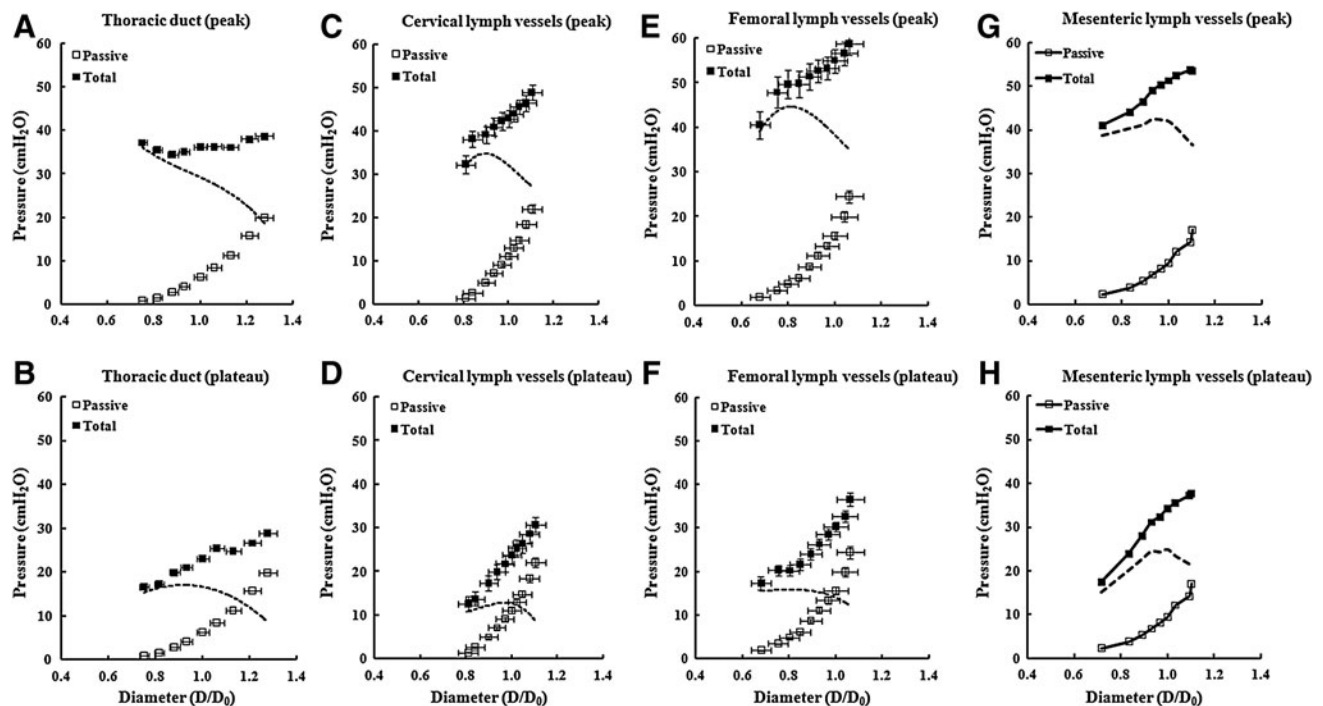
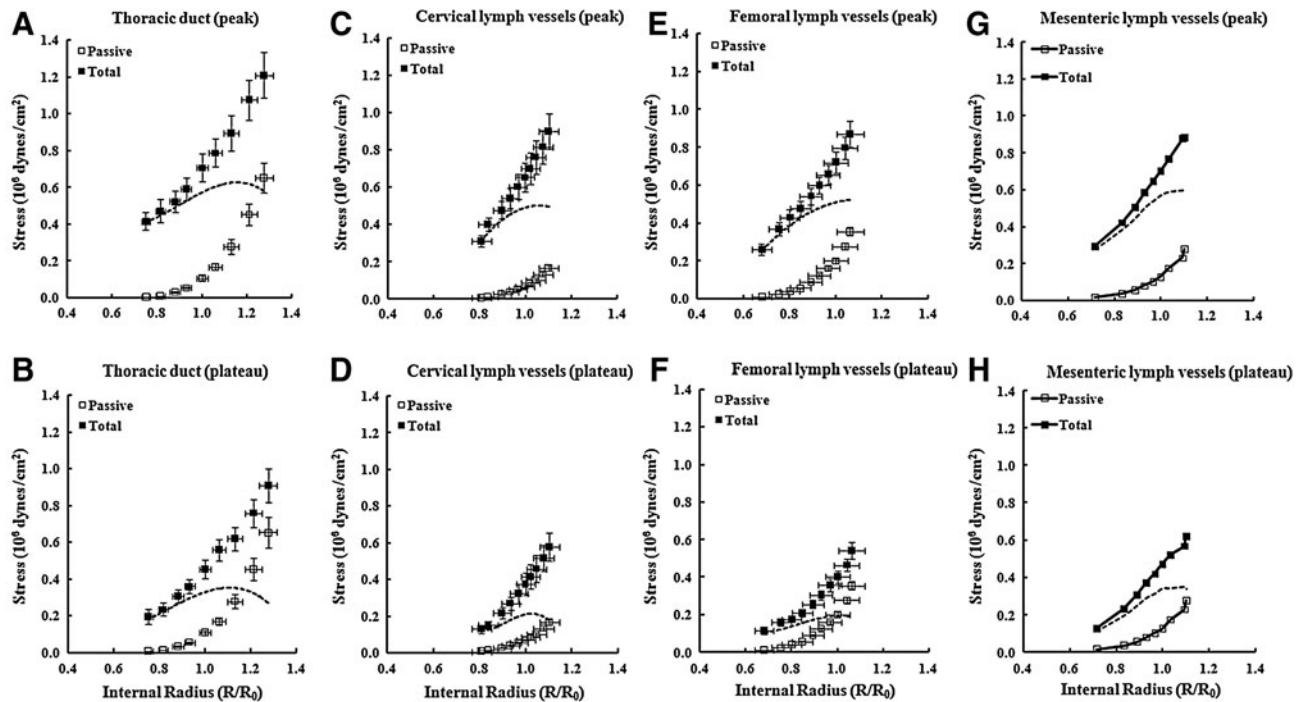


FIG. 2. Calculated pressure as a function of normalized diameter for lymph vessels from four different regions.  $\square$ , Calculated pressure in passive vessels;  $\blacksquare$ , calculated pressure in activated vessels (total pressure).  $D/D_0$  is normalized diameter, where  $D_0$  is the diameter associated with maximal active force. The *dashed line* indicates the pressure calculated from active tension. Error bars,  $\pm$ SEM. Data from mesenteric lymph vessels is re-plotted from Ref. 11 for comparison.



**FIG. 3.** Wall stress as a function of normalized internal radius for lymph vessels from four different regions.  $\square$ , Wall stress in passive vessels;  $\blacksquare$ , wall stress in activated vessels (total stress).  $R/R_0$  is the normalized internal radius, where  $R_0$  is the radius associated with maximal active force. Active stress (dashed line) was obtained by subtracting the passive curve from the activated curve. Error bars,  $\pm$  SEM. Data from mesenteric lymph vessels is re-plotted from Ref. 11 for comparison.

the experiments, and wall stress was computed by dividing wall tension by wall thickness of the media layer at each point on the length–tension curve. For mesenteric lymph vessels, the wall thickness averaged  $6.0 \pm 0.7 \mu\text{m}$ .<sup>11</sup> Wall stress was then plotted as a function of the normalized radius,  $R/R_0$ , where  $R$  and  $R_0$  were the internal radii calculated from  $L$  and  $L_0$ . Maximal active wall stress was estimated by subtracting the passive curve (open squares) from the total curve (closed squares).

For all three vessel types, the optimal preloads corresponding to the maximal active stresses were shifted slightly to the right in comparison to the optimal preloads for the respective maximal active tensions (Fig. 1). Maximal active stresses at the peaks of contraction were all within  $\sim 20\%$  for the four lymph vessel types. There was more variability in the values of maximal active stress for the plateau phase of contraction, with cervical and femoral vessels being lowest, and thoracic duct and mesenteric lymph vessels being about 80% higher.

## Discussion

We proposed previously that regional differences in the sensitivity of lymph vessels to increases in transmural pressure or stretch reflect differences in the ability of lymphatic muscle to regulate force development according to local hydrodynamic conditions. The basic length–tension relationships of vessels from the four different lymphatic regions shown in Figure 1 are consistent with this hypothesis. In this regard, at least three aspects of our findings are notable. 1) All groups of vessels had relatively broad plateaus in their active tension versus length relationships, suggesting that they are adapted to generate near-maximal tensions over a relatively wide range of

preloads (at least  $0.85\text{--}1.05 L_0$ ). This would allow the vessels to adapt or maintain their contractile properties in the face of highly variable local combinations of transmural pressures and intraluminal flows that are known to occur in the lymphatic system.<sup>17,18</sup> 2) The thoracic duct exhibited the flattest active tension curve, particularly for peak active tension, in which there was less than a 5% change in peak active tension from  $0.75$  to  $1.3 L_0$ . This finding supports earlier conclusions of a relatively greater conductive function for this major lymphatic trunk in the body compared to other parts of the lymphatic system, allowing the thoracic duct to remain relatively insensitive to changes in pressure and more likely to be regulated primarily by changes in flow.<sup>13</sup> Changes in the tone of the duct are important to regulate its ability to lower local resistance during periods of high flow;<sup>6</sup> therefore comparatively similar values of active tension at different preloads may establish conditions for a similar contractile response to a wide range of changes in filling of the duct. This characteristic of the thoracic duct may also minimize myogenic constriction<sup>19</sup> at times when flow is high enough to move lymph passively through it; otherwise contractile activation would increase its resistance to flow.<sup>6,18</sup> 3) Femoral lymph vessels were able to withstand the highest pressures, followed by mesenteric and cervical vessels, and then thoracic duct. We propose that this hierarchy reflects the existence of periods of higher transmural pressures and resistances to flow in femoral lymphatic network, which imposes greater demands to the contractile ability of the femoral lymph vessels. At the other end of the spectrum is the thoracic duct with its lower resistance to flow.

To make comparisons between the isometric measurements made in the present study and isobaric measurements

of the optimal pressure range for pumping made in a previous study,<sup>13</sup> we calculated the maximal pressures the four types of vessels would be able to withstand under conditions when the lymphatic muscle was maximally activated (Fig. 2). Femoral lymph vessels were able to withstand the highest estimated pressures (~45 cm H<sub>2</sub>O), followed by mesenteric (~40 cm H<sub>2</sub>O) and cervical vessels (~35 cm H<sub>2</sub>O), and then thoracic duct (~35 cm H<sub>2</sub>O). It is probably not coincidental that this rank order probably reflects the relative levels of hydrostatic pressure normally experienced by these vessels. Mesenteric vessels would experience relatively higher pressures in the portal circulation and femoral vessels would be more subject to gravitational loads incurred with changes in body position. Femoral and mesenteric lymph vessels also have higher outflow resistances because they are located further upstream in their respective lymphatic vascular networks than cervical lymph vessels or thoracic duct.

Finally, we can speculate that the same relative relationships would hold for lymph vessels in bipeds or other mammals whose extremities are routinely subjected to gravitational loads. Indeed, the maximal active tensions and pressures in lymph vessels from dependent extremities would be predicted to be even greater than those in rat femoral lymph vessels. The rat is a quadruped that experiences hydrostatic loads (due to gravity) of only a few cm H<sub>2</sub>O in the various body positions encountered during normal activities. In bipeds, potentially much greater hydrostatic loads are presumably ameliorated by the secondary, intraluminal valve system (if the valves are functional), but relatively high hydrostatic pressures have nevertheless been recorded in lymph vessels in both normal and diseased human extremities when a limb is placed in a dependent position.<sup>12,20,21</sup> Lymph vessels in dependent extremities probably must be able generate relatively robust levels of active tension in the muscle layer to prevent the overdistention that would otherwise lead to weakening of the wall and eventually to chronic inflammatory processes.

In conclusion, these are the first comparative measurements and analyses of the basic length-tension relationships in lymph vessels from four different regions—thoracic duct, cervical, mesenteric and femoral lymph vessels. We surmise that lymph vessels effectively adapt their contractile force to the particular hydrodynamic conditions (transmural pressures and intraluminal flows) that exist in different regions of the lymphatic system.

#### Authors Disclosure Statement

No competing financial interests exist.

#### References

- Mazzoni MC, Skalak TC, Schmid-Schonbein GW. Structure of lymphatic valves in the spinotrapezius muscle of the rat. *Blood Vessels* 1987;24:304–312.
- Schmid-Schonbein GW. Microlymphatics and lymph flow. *Physiol Rev* 1990;70:987–1028.
- Gashev AA. Lymphatic vessels: Pressure- and flow-dependent regulatory reactions. *Ann NY Acad Sci* 2008;1131:100–109.
- Mislin H, Rathenow D. Experimentelle Untersuchungen über die bewegungskoordination der Lymphangione. [In German]. *Revue Suisse Zool* 1962;69:334–444.
- Dixon JB, Greiner ST, Gashev AA, Cote GL, Moore JE, Zawieja DC. Lymph flow, shear stress, and lymphocyte velocity in rat

- mesenteric prenodal lymphatics. *Microcirculation* 2006;13:597–610.
- Gasheva OY, Zawieja DC, Gashev AA. Contraction-initiated NO-dependent lymphatic relaxation: A self-regulatory mechanism in rat thoracic duct. *J Physiol* 2006;575:821–832.
- Muthuchamy M, Zawieja D. Molecular regulation of lymphatic contractility. *Ann NY Acad Sci* 2008;1131:89–99.
- Benoit JN, Zawieja DC, Goodman AH, Granger HJ. Characterization of intact mesenteric lymphatic pump and its responsiveness to acute edemagenic stress. *Am J Physiol* 1989;257:H2059–2069.
- Eisenhoffer J, Elias RM, Johnston MG. Effect of outflow pressure on lymphatic pumping *in vitro*. *Am J Physiol* 1993;265:R97–102.
- Zhang R, Gashev AA, Zawieja DC, Lane MM, Davis MJ. Length-dependence of lymphatic phasic contractile activity under isometric and isobaric conditions. *Microcirculation* 2007;14:613–625.
- Zhang RZ, Gashev AA, Zawieja DC, Davis MJ. Length-tension relationships of small arteries, veins, and lymphatics from the rat mesenteric microcirculation. *Am J Physiol Heart Circ Physiol* 2007;292:H1943–1952.
- Olszewski WL, Engeset A. Intrinsic contractility of prenodal lymph vessels and lymph flow in human leg. *Am J Physiol* 1980;239:H775–783.
- Gashev AA, Davis MJ, Delp MD, Zawieja DC. Regional variations of contractile activity in isolated rat lymphatics. *Microcirculation* 2004;11:477–492.
- Mulvany MJ. Procedures for investigation of small vessels using a small vessel myograph. Aarhus, Denmark: Danish Myo Technology, 2003.
- Gore RW. Wall stress: A determinant of regional differences in response of frog microvessels to norepinephrine. *Am J Physiol* 1972;222:82–91.
- Schubert R, Wesselman JP, Nilsson H, Mulvany MJ. Norepinephrine-induced depolarization is smaller in isobaric compared to isometric preparations of rat mesenteric small arteries. *Pflügers Arch* 1996;431:794–796.
- Gashev AA. Basic mechanisms controlling lymph transport in the mesenteric lymphatic net. *Ann NY Acad Sci* 2010;1207:E16–20.
- Gashev AA, Zawieja DC. Hydrodynamic regulation of lymphatic transport and the impact of aging. *Pathophysiology* 2010;17:277–287.
- Davis MJ, Davis AM, Ku CW, Gashev AA. Myogenic constriction and dilation of isolated lymphatic vessels. *Am J Physiol Heart Circ Physiol* 2009;296:H293–302.
- Olszewski WL. Contractility patterns of normal and pathologically changed human lymphatics. *Ann NY Acad Sci* 2002;979:52–63; discussion 76–79.
- Saul ME, Thomas PA, Dosen PJ, Isbister GK, O'Leary MA, Whyte IM, McFadden SA, van Heiden DF. A pharmacological approach to first aid treatment for snakebite. *Nature Med* 2011;17:809–811.

Address correspondence to:

Anatoliy A. Gashev, M.D., Ph.D., D.Med.Sci.

Department of Systems Biology and Translational Medicine

College of Medicine

Texas A&M Health Science Center

702 SW H.K. Dodgen Loop

Temple, TX 76504

E-mail: gashev@tamuedu